

# Wettability Alteration of Carbonate Reservoirs Using Imidazolium-Based Ionic Liquids

Sivabalan Sakthivel\*

Cite This: *ACS Omega* 2021, 6, 30315–30326

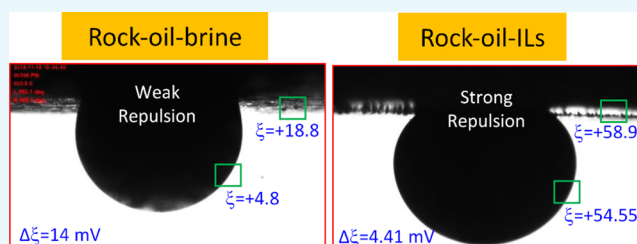
Read Online

ACCESS |

Metrics &amp; More

Article Recommendations

**ABSTRACT:** The wettability of the rock–oil–brine system plays a major role in enhanced oil recovery (EOR), particularly in the harsh environments of carbonate reservoirs. Most of these formations were identified as strongly oil-wet, and sometimes a few are intermediate-wet. Hence, it is highly necessary to alter such an oil-wet rock matrix to a water-wet matrix in order to improve the oil production. Consequently, it is important to investigate the wetting and wettability dynamics of the rock–oil–brine system for both static and dynamic cases. Thus, in this study, we investigated the effect of four various imidazolium-based ionic liquids (ILs) on the wettability alteration of the rock–oil–brine system by measuring the contact angles. Herein, we have screened various parameters, such as the rock type (brine-saturated and oil-saturated), type of IL, IL concentrations (0–1000 ppm), temperature (25–100 °C), pressure (14.7–3000 psi), and salinity (TDS: 67,500–240,000 ppm). The measurement of the static contact angle was found to be altered from 85.5 to 49.4° with the addition of 500 ppm of ILs in the brine-saturated sample, and for the oil-saturated sample, it was altered from 150.9 to 99.2°. This indicates that ILs have a huge influence on shifting the rock wettability more toward water-wet, which in fact is more favorable for the EOR operation. Later, we studied the dynamic wettability alteration of the rock–oil–brine system, in which we measured the transient changes in the contact angle while displacing the brine with an IL solution in situ. It was observed that the oil droplet deformed slightly and was dragged toward the base fluid (IL solution) with time, and this implied the changes in the contact angle from 150.9 to 118.5° with 500 ppm of IL,  $[C_{12}mim]^+[Cl]^-$ . Though this has a relatively lesser impact as compared to the static experiment, this could be considered to be more realistic to correlate with coreflood experiments. Further, to understand the mechanism of this wettability dynamics, we have measured the oil–water interfacial tension and the  $\zeta$ -potential of various systems and observed that their results were backed up by our wettability studies. Overall, the combined forces of interfacial tension reduction, capillary alterations, and IL interactions with rocks and oils have caused this wettability alteration. Conclusively, the results of various experiments that are performed in this study are more meaningful, and it is evident that ILs favor the successful EOR implications.



## 1. INTRODUCTION

Two-thirds of the world's oil reserves are matured and unrecovered even after the conventional primary and secondary recovery operations. Interfacial science plays a major role in the process of enhanced oil recovery (EOR), wherein specialized chemicals are used in order to alter the physical properties of the reservoir's environment, which accelerates the tertiary recovery. The detachment and mobility of the trapped or bypassed residual oils are mainly influenced by key factors, namely, the capillary force, viscous force, contact angle, wettability, surface tension, interfacial tension, and so forth.<sup>1</sup> Among these factors, wettability is the most governing factor, which can be defined as the comparative adhesive force of two different immiscible fluids on a solid surface.<sup>2,3</sup> Wettability is one of the crucial factors that has the potential ability to control oil productivity and relative permeability and estimate the fluids in the reservoir. Measuring the surface contact angle of the rock–oil–water system is one of the most often used wettability assessing methods in the industry due to its least complexity, wherein the macroscopic

contact angle of oil adherence is used to be measured. Recently, it has been estimated that nearly more than half of the world's reservoirs are categorized as carbonate formations in which 90% of them are identified as oil-wet, and, in rare cases, a few of them are intermediate-wet.<sup>1</sup> It is highly recommended and also a prerequisite to alter this native oil-wet state to a water-wet state or close to a water-wet state so as to mobilize the residual or bypassed oil toward the production well. Typically, the injection of specialized oilfield chemicals would facilitate such wettability modification and thus improve the oil production. Typically, surfactants, nanofluids, alkali, smart (low-salinity) brines, or a

Received: May 29, 2021  
Accepted: October 21, 2021  
Published: November 1, 2021



combination of two or more of these are employed as wettability modifiers. These wettability modifiers facilitate the EOR by detaching the high-capillary oil blobs. In general, it is the modification of physical or chemical interactions (forces) that are acting on the rock–oil–water systems.<sup>4</sup> However, it varies depending on various factors, such as the rock type, pH, oil composition, soaking time, temperature, pressure, salinity, and so forth.<sup>5,6</sup>

However, in the last couple of decades, many researchers have studied the efficiency of various surface-active agents (surfactants, polymers, nanofluids, alkali, etc.) in oil recovery. Most of these studies were performed at lower temperatures and in zero or lesser salinity, unlike the reservoir conditions. Though, the use of surfactants and nanofluids is more efficient, unfortunately, many of these chemicals fail to perform in harsh environments (high temperature, high salinity, and high pressure). The conventional oilfield surfactants and nanofluids lacked their colloidal stability at the resident brine and temperature conditions of the reservoir, which causes severe formation damage by precipitation and plugging of the pores and throats.<sup>9–28</sup> Recently, several stable specialized oilfield chemicals (Gemini surfactants, carbon nanotubes, etc.) have been developed and tested to identify their implications in oil recovery, even at harsh temperatures and salinity. However, in the case of field study, the usage of such expensive chemicals in a larger quantity and also in high concentrations cannot be considered as economically viable.

Recently, the newly developed ionic liquids (ILs) have emerged as green solvents. ILs are a kind of organic molten salts that poorly coordinated with organic cations and organic or inorganic anions; typically, they are found in the liquid state at ambient conditions or below 100 °C. They also exhibit excellent physicochemical properties, such as a low melting point, negligible vapor pressure, no flammability, high solvation capability, high colloidal stability (both thermally and chemically), and so forth.<sup>7,8</sup> Since they have negligible or no vapor pressure, they are also considered as eco-efficient, unlike the typical organic solvents. Moreover, ILs can be recycled and reused several times; hence, they can be considered as the best alternatives to the conventionally used oilfield chemicals.<sup>9</sup> Recently, many researchers have investigated the implication of ILs in oilfield applications, such as bitumen dissolution, de-asphalting, interfacial tension (IFT) reduction, oil displacement efficiency, and so forth.<sup>9–28</sup>

In the recent past, we have studied several ILs, such as imidazolium-, alkyl ammonium-, and lactam-based ILs, to investigate oil–water IFT reduction, heavy oil upgradation, oil recovery on the sand-pack column, and so forth. However, all these were studied at below 60 °C and in zero or low salinity using a monovalent salt, NaCl. A significant reduction of oil–water IFT was observed with the addition of a minor quantity of ILs. Overall, the longer chain length ILs showed better efficiency on IFT reduction than the shorter chain length ILs.<sup>11–18,25–28</sup> Though many ILs were screened for oil–water IFT, none were studied at the resident brine condition (multivalent ionic composition); instead, a single salt with low salinity and low temperature alone was covered.<sup>11–18,25–28</sup>

Bin Dahbag et al. (2015) investigated a few of the conventional ammonium-based ILs for the measurement of static wettability on the Berea sandstone at 60 °C and in 2000 psi. It was noted that there is an alteration of static wettability from oil-wet state to medium water-wet state upon increasing the IL concentrations from 0 to 1000 ppm.<sup>29</sup> Cao et al. (2017)

investigated the effect of imidazolium-based borate ILs (1-ethyl-2,3-dimethylimidazolium tetrafluoroborate, 1-ethyl-3-methylimidazolium tetrafluoroborate, 1-butyl-3-methylimidazolium tetrafluoroborate, and 1-butyl-2,3-dimethylimidazolium tetrafluoroborate) for the static wettability studies on different solid surfaces such as mica, limestone, sandstone, and so forth. A better efficiency with borate ILs on altering wettability from 100 to 50° was observed with the use of high-concentration (1 wt %) ILs.<sup>30</sup> Nabipour et al. (2017) investigated the ability of two imidazolium-based ILs ( $[\text{C}_{12}\text{mim}]^+[\text{Cl}]^-$  and  $[\text{C}_{18}\text{mim}]^+[\text{Cl}]^-$ ) for the study of wettability alteration and oil recovery performances on the Iranian carbonate reservoir at ambient conditions. They successfully demonstrated the static wettability alterations and observed about 8–22% of increased oil recovery with ILs.<sup>31</sup> Abdullah et al. (2017) investigated some of the polyionic liquids on the Berea sandstone for wettability and oil recovery performances at 60 °C and in 2000 psi. It was noted that the surface wettability of the rock sample was altered from 120 to 50° upon using ILs. Subsequently, the coreflood experiment of the same demonstrated about 8–9% of additional oil recovery over the simple waterflooding.<sup>32</sup> In the same way, Pillai et al. (2018) investigated the efficacy of three imidazolium-based ILs (1-octyl-3-methylimidazolium tetrafluoroborate, 1-decyl-3-methylimidazolium tetrafluoroborate, and 1-dodecyl-3-methylimidazolium tetrafluoroborate) on the oil-saturated quartz surface for the study of wettability measurements on the rock–water–air system with and without ILs at ambient conditions. They observed a positive indication of the wettability alteration toward water-wet state upon increasing the IL concentration.<sup>13</sup> Similarly, Pillai and Mandal (2020) also investigated the poly [1-hexadecyl-3-vinyl-imidazolium bromide] IL on the sandstone samples for the study of wettability and oil recovery processes at ambient conditions. In both cases, they studied only the rock–water–air instead of the rock–oil–water condition. However, they noted an increase in water-wet characteristics upon increasing the IL concentrations and also quantified its impact on the coreflood oil recovery.<sup>14</sup> Additionally, it can also be noted that most of the studies were performed at relatively low temperature and low salinity (ambient conditions), unlike the reservoir conditions.

Albeit many researchers have studied the efficacy of ILs on sandstone and quartz surfaces, only very limited studies are found on carbonate. Additionally, most studies were carried out only on a simple rock–water–air contact angle system instead of the rock–oil–water three-phase system. Also, most experiments were conducted at a low temperature and low or no salinity, which fail to represent the realistic reservoir conditions. Additionally, there are no dynamic wettability studies found in the open literature for the case of ILs. Hence, it is necessary to investigate the impact of ILs on the most abundant carbonate reservoirs at the reservoir conditions (at high temperature, 100 °C, and high salinity, TDS 240,000 ppm). Consequently, it is also necessary to investigate the dynamic wettability that would be more useful to correlate to the oil recovery performances over the IL injections. Besides, this is a costlier chemical and impractical method to use at high concentrations (0.5–2 wt %) in the case of field studies; thus, it is essential to optimize the studies with the least optimum concentrations.

The objective of this study is to investigate the efficacy of imidazolium-based ILs for the study of wettability dynamics on carbonate reservoirs at high temperature and high salinity. Herein, we determined the wettability of the rock–oil–water system as a function of various factors such as the type of IL, the

Table 1. SARA Analysis of the Crude Oil Sample

saturates	composition (wt %)			API gravity	density (kg/m <sup>3</sup> ) at 25 °C	viscosity (cP) at 25 °C
	aromatics	resins	asphaltenes			
36.2	50.0	11.0	2.8	28.75	0.8724	15.1

Table 2. List of Used ILs in This Study

Cation	Anion	Name	Abbreviation
	[Cl] <sup>-</sup>	1-butyl-3-methylimidazolium chloride	[C <sub>4</sub> mim] <sup>+</sup> [Cl] <sup>-</sup>
	[Cl] <sup>-</sup>	1-hexyl-3-methylimidazolium chloride	[C <sub>6</sub> mim] <sup>+</sup> [Cl] <sup>-</sup>
	[Cl] <sup>-</sup>	1-octyl-3-methylimidazolium chloride	[C <sub>8</sub> mim] <sup>+</sup> [Cl] <sup>-</sup>
	[Cl] <sup>-</sup>	1-decyl-3-methylimidazolium chloride	[C <sub>12</sub> mim] <sup>+</sup> [Cl] <sup>-</sup>

type of rock (oil-saturated or brine-saturated), concentrations (0–500 ppm), aging duration, temperature (25–100 °C), pressure (14.7–3000 psig), and salinity (TDS: 67,500–240,000 ppm). This study intends to represent Saudi Arabian reservoir conditions; henceforth, we executed this study at a high temperature, a high pressure, and a high salinity. In this study, we employed two various rock samples, one is seawater-saturated and another one is oil-saturated. Four various imidazolium-based ILs were screened as a function of alkyl chain length. Here, we have demonstrated both the static and dynamic responses of imidazolium ILs on the rock–oil–water wettability, which are more relevant and essential prerequisites for the better performances of EOR operations. After this, we also measured the oil–water IFT and the  $\zeta$ -potential of various colloidal systems to furnish further insights to support the wettability mechanism. Later, the mechanism for these wettability alterations using ILs is discussed with the aid of experimental results.

## 2. EXPERIMENTAL SECTION

**2.1. Materials: Crude Oil, ILs, Surfactants, Brine Fluids, and Core Samples.** In this study, we used the Saudi Arabian crude oil sample. The physicochemical properties (viscosity, density, and SARA analysis) of the oil sample are shown in Table 1. It contains more aromatics and saturates and the less amount of resins and asphaltenes as well (36.2% saturates, 50% aromatics, 11% resin, and 2.8% asphaltenes).

Four imidazolium-based ILs, namely, 1-butyl-3-methylimidazolium chloride [C<sub>4</sub>mim]<sup>+</sup>[Cl]<sup>-</sup>, 1-hexyl-3-methylimidazolium chloride [C<sub>6</sub>mim]<sup>+</sup>[Cl]<sup>-</sup>, 1-octyl-3-methylimidazolium chloride [C<sub>8</sub>mim]<sup>+</sup>[Cl]<sup>-</sup>, and 1-decyl-3-methylimidazolium chloride [C<sub>12</sub>mim]<sup>+</sup>[Cl]<sup>-</sup>, were purchased from Sigma-Aldrich and used as such with no further analysis. Table 2 shows the chemical structure of the used ILs with their proper abbreviations. Herein, we also investigated one commonly used surfactant (alpha-olefin sulfonate, AOS) as a reference case so that the efficiency of ILs can be evaluated over the simple surfactant. AOS is the most conventionally used anionic surfactant in the oilfield industry, and therefore, we used it as a reference.

Most of the Middle East reservoirs are highly saline formations with a large quantity of mono- and divalent ions, which also vary from one region to other. Therefore, we formulated three different types of brine solutions based on the field report. They are seawater (SW) 67,500 ppm, low-salinity formation water (LS) 138,000 ppm, and high-salinity formation water (FW) 241,000 ppm. The chemical compositions of all the brine fluids are summarized in Table 3.

Table 3. Chemical Composition of the Formulated Seawater, Low-Salinity Formation Water, and High-Salinity Formation Water

salt	seawater (SW) g/L	low-salinity formation water (LS) g/L	high-salinity formation water (FW) g/L
NaCl	41.042	75.223	150.446
CaCl <sub>2</sub> ·2H <sub>2</sub> O	2.385	34.920	69.841
MgCl <sub>2</sub> ·6H <sub>2</sub> O	17.645	10.198	20.396
Na <sub>2</sub> SO <sub>4</sub>	6.343	0.259	0.518
NaHCO <sub>3</sub>	0.165	0.2435	0.487

For this study, we used Indiana limestone core samples. Typically, Saudi Arabian reservoirs are rich in carbonate. Thus, we employed the Indiana limestone, which has a very similar mineral composition to the Saudi Arabian oilfield. Herein, we sliced 40 pieces of disc-shaped core samples (1 in. diameter and 35 mm thickness) from the larger core plug of Indiana limestone. All these slices were cleaned in the Dean-Stark apparatus using toluene/methanol as the solvents and dried thoroughly at 100 °C for 24 h. Later, the samples were divided into two portions in order to prepare different types of samples (oil wet and water wet). First, half of the cleaned core slices were subjected to saturate in seawater and the remaining half of the samples were saturated in crude oil under vacuum at a pressure of 3000 psi at their corresponding medium. Later, they were aged in the oven (at 100 °C) for different time durations (0, 7, and 14 day). The mineral composition of the rock samples was found to be more of calcium carbonate (>97%). The average petrophysical properties of the core samples are briefed in Table 4.



Table 4. Petrophysical Properties of the Disc-Shaped Core Samples Used for Wettability Experiments

rock type	length (cm)	width (cm)	pore volume (mL)	porosity (%)	permeability (mD)	
					gas (He)	brine (SW)
Indiana limestone (outcrop)	0.35	2.522	0.351	19.09	271.3	203.0

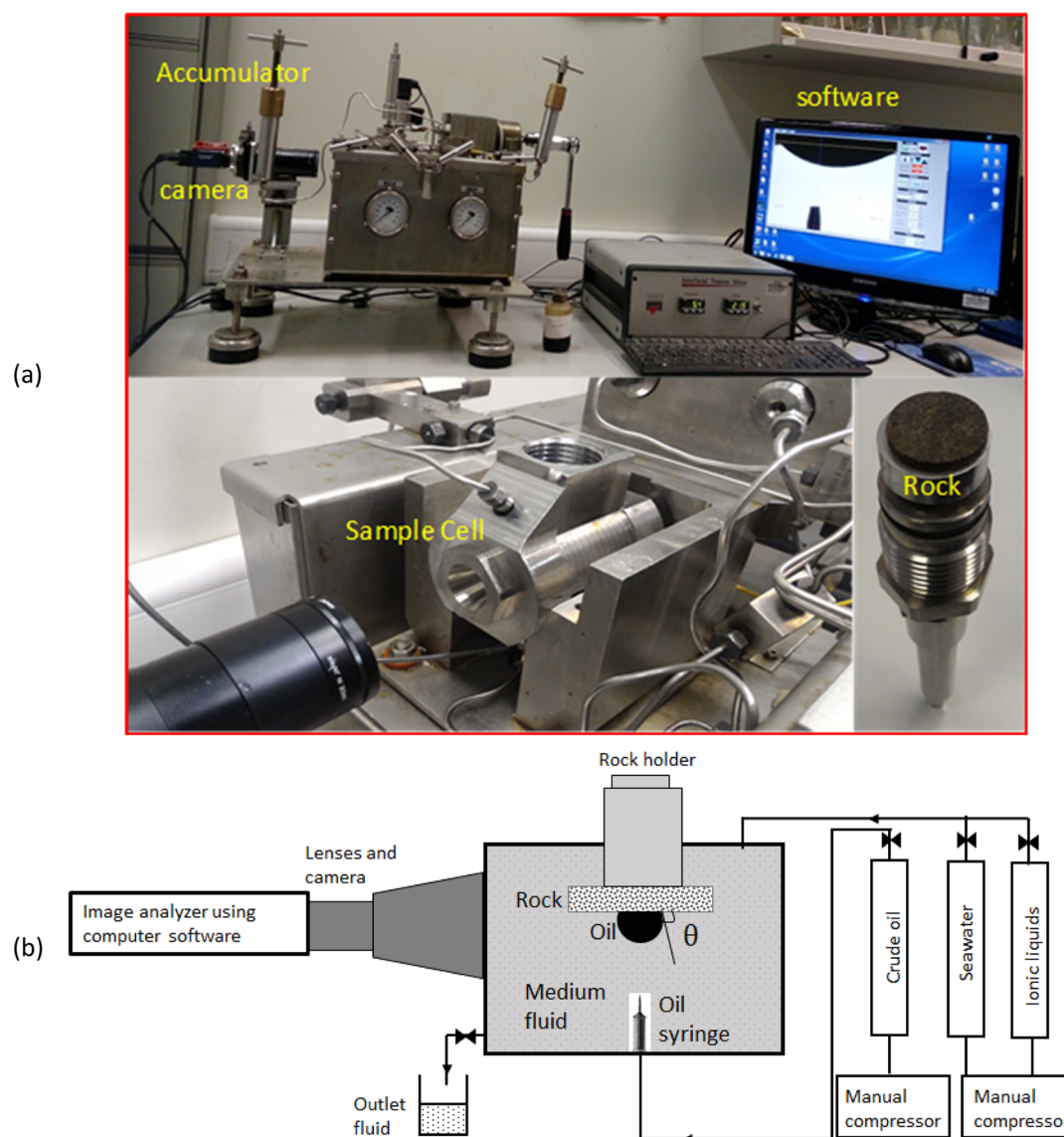
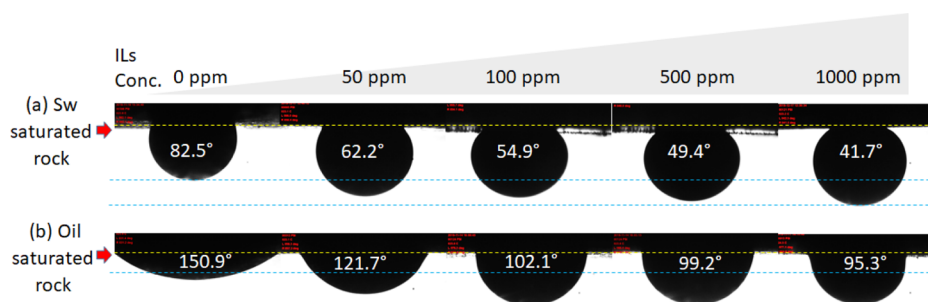


Figure 1. (a) Photograph, (b) schematic of the high-pressure high-temperature (HPHT) tensiometer.

**2.2. Experimental Methods. 2.2.1. Static Wettability.** Figure 1 shows the photograph and schematic of the experimental setup (Interfacial Tension Meter, IFT-700, Vinci Tech) used for our study. As depicted in Figure 1a,b, we used the invert sessile drop method to measure the contact angle of the rock–oil–brine systems. It consists of a rock holder, a syringe/needle loaded with crude oil, a fluid cell holder (optically transparent) to fill the brine fluid, temperature controller (thermostat), accumulators for oil/brine storage, a pressurizing system through fluid compression, a high-resolution digital camera for imaging, and an in-built software for image analysis. Initially, the desired base or brine fluid was loaded into the fluid cell holder; later, the brine- or oil-saturated rock sample was mounted on the stainless steel rock holder; it is then suspended into the brine fluid for about 30–60 min to equilibrate with brine. The crude oil-loaded needle is placed at the bottom of the

fluid cell holder. Thereafter, the desired temperature and pressure of the system are set and allowed to stabilize for about an hour. Afterward, the oil droplet was generated using a syringe and landed at the bottom of the suspended rock surface. It was allowed to stabilize for a while (15–30 min), and then the rock–oil–brine contact angle was measured through the denser phase (brine) of the digital image that was captured using the in-built IFT-700 software. An identical procedure was followed for all the subsequent fluids, such as SW, LS, FW, SW + IL, SW + AOS, and so forth. Correspondingly, three different types of brines (SW, LS, and FW) were studied with and without ILs:  $[C_4\text{mim}]^+[\text{Cl}]^-$ ,  $[C_6\text{mim}]^+[\text{Cl}]^-$ ,  $[C_6\text{mim}]^+[\text{Cl}]^-$ , and  $[C_{12}\text{mim}]^+[\text{Cl}]^-$ . All these experiments were studied at four different temperatures (25, 50, 75, and 100 °C) and four different pressures (14.7, 1000, 2000, and 3000 psig). All these



**Figure 2.** Effect of different concentrations of IL,  $[C_{12}mim]^+[Cl]^-$ , on the contact angle measurement of the oil–rock–seawater system for both (a) brine-saturated and (b) oil-saturated rocks at 25 °C.

experiments were replicated thrice or more, and the average was reported.

**2.2.2. Dynamic Wettability.** Although the static contact angle measurements are more informative, which reveals the state of the rock's wetting, it is not so realistic as the wettability transition takes place during the chemical flooding in the EOR. In static wettability, the rock surfaces are exposed to the IL solutions before landing of the oil drop on the rock surface; hence, their results cannot be directly correlated with the flooding performances. In the typical EOR experiments, first, the rock sample was first saturated with crude oil, and then the conventional waterflooding will be initiated. Once it reaches the water cut, injection of chemical agents would be implemented to alter the rock wettability and thus to increase the oil recovery, which is completely different from what we assess in static wettability. To emulate the realistic reservoir wettability modification, we have done some modifications on the IFT-700 setup<sup>33</sup> and studied the dynamic wettability.<sup>34–36</sup> In that, the oil was landed on the rock surface through a brine medium, as stated before in static wettability. Later, the base fluid (brine) of this system was replaced with the continuous injection of new chemical solutions (ILs) with a very slow injection rate (2–4 cc/min) to obtain the transient dynamic wettability. The injection was continued until the desired concentration of the ILs reaches the cell holder, and it was confirmed by measuring the UV–vis absorption of the inlet and outlet effluents. Once the outlet absorption reaches the injection fluid absorption, it is assumed that the cell holder reached the desired concentration of the IL solution. Thereafter, the change in contact angle was analyzed for the next 24 h. The measurement of contact angle before and after IL injection was documented for better understanding of the effect of IL dynamics on carbonate rock wettability alteration.

**2.2.3. Interfacial Tension Measurements.** The interfacial tension of various oil–water systems was studied using the same instrument, Interfacial Tension Meter (IFT-700, Vinci Tech), in which the effect of ILs was screened as a function of IL concentration using the pendant drop method. In this method, the maximum shape of the oil droplet was suspended into the bulk fluid and the interfacial forces based on the drop shape analysis were measured.<sup>37</sup>

**2.2.4. Zeta Potential Measurements.** A  $\zeta$ -potential analyzer (Dispersion Tech Inc. 1202: Acoustic and Electroacoustic spectrometer) was employed to measure the  $\zeta$ -potential of various colloidal systems, such as rock + DI, rock + SW, rock + ILs + SW, oil + DI, oil + ILs, and rock + ILs + SW systems. Initially, 0.1 g of the milled carbonate rock powders (100–200  $\mu$ m size) was dispersed in 10 mL of various base fluids, sonicated for about 1–2 h at 40 kHz, and allowed to rest for 10–12 h to

reach the equilibrium. In the same way, we prepared the oil-suspended emulsion by mixing 0.1 g of oil sample in 10 mL of base fluid, followed by vigorous shaking (10–12 h) and sonication (1–2 h). After that, it was allowed to rest for 10–12 h. Third, a mixture of rock + oil + brine was prepared with and without ILs. This one just provides the average  $\zeta$ -potential of rock, oil, and ILs; hence, it cannot be directly correlated with rock or oil, unlike the rock/brine and oil/brine systems. All these prepared solutions showed the pH in the range of 7.39–7.67. This is very similar to the reservoir pH. Thus, no pH alteration was attempted. Later, the required amount of the sample (about 5 mL) was loaded into the sample holder and the  $\zeta$ -potential of rock/brine and oil/brine interfaces with and without ILs was measured. Therein, the in-built platinum electrodes were placed in the sample holder. All these measurements were conducted at 25 and 80 °C.

The frequency of the applied electrical field was set automatically based on the conductivity of the fluids. All these measurements were repeated thrice in order to ensure reproducibility and their average was reported.

### 3. RESULTS AND DISCUSSION

The first part of this section discusses the measurements of static wettability of rock–oil–brine systems with and without ILs. This study was covered as a function of rock type, IL type, IL concentrations (0–1000 ppm), salinity (TDS: 67,500–240,000 ppm), temperature (25–100 °C), and pressure (14.7–3000 psig). Second, the measurement of wettability alteration was demonstrated dynamically with the continuous injection of IL solutions on the pre-generated oil droplet on the rock–oil–SW system. This mimics the realistic wettability modification that takes place during the process of coreflood at high pressure and high temperature. Finally, this study discusses the  $\zeta$ -potential of the rock sample dispersion in the different base fluids with and without ILs. Indeed, these  $\zeta$ -potential measurements provide a good insight to understand the wettability mechanism.

**3.1. Static Wettability. 3.1.1. Effect of IL Concentrations.** As stated in Section 2.1.2, two types of rock samples were employed in this study: (i) seawater-saturated rock and (ii) oil-saturated rock. First, the effect of various concentrations of IL,  $[C_{12}mim]^+[Cl]^-$ , were studied for the static wettability at 25 °C and 14.7 psig. Figure 2 shows the effect of different concentrations of IL,  $[C_{12}mim]^+[Cl]^-$ , on the static contact angle of the rock–oil–seawater system for both the brine- and oil-saturated samples. All these screened samples in this study are unaged. First, the seawater-saturated sample was studied for the baseline experiment without ILs. The measured contact angle was found to be mostly neutral or intermediate-wet as 82.5° (refer to the first row at Figure 2). The addition of IL,

$[C_{12}mim]^+[Cl]^-$ , on the same system, shifted the wetting characteristics more toward water-wet. Here, five different concentrations of ILs, namely, 0, 50, 100, 500, and 1000 ppm, were studied, and their contact angles were found to be 82.5, 62.2, 54.9, 49.4, and 41.7°, respectively. In the same way, the same set of experiments were repeated for the oil-saturated rock sample at the same experimental conditions and their results are displayed in the second row of Figure 2. Here, the baseline experiment of the rock–oil–seawater system shows a contact angle of 150.9°, which indicates that it has strong oil-wet characteristics. The same system with the addition of 0, 50, 100, 500, and 1000 ppm of ILs altered the surface contact angles to 150.9, 121.7, 102.1, 99.2, and 95.3°, respectively. It is a strong indication that ILs alter the rock wettability more favorably toward the neutral-wet or intermediate-wet from its native oil-wet characteristics. However, ILs are efficient in all the studied systems, which are more dominant in the water-wet sample than in the oil-wet samples. For instance, in the brine-saturated sample, wetting was altered from 82.5 to 41.7° with 500 ppm of ILs, which is about 49% of wettability reduction, whereas in the case of oil-saturated sample, wetting was altered from 150.9 to 95.3°, which is about 37% of reduction. This is due to the existence of additional hydrophobic interactions that are exhibited in the oil-wet sample between the oil-adsorbed rock surface and the landed oil droplet, which is not the case in brine-saturated water-wet samples. It was even reflected with the addition of ILs. This leads to the variation in the degree of wettability alteration between oil-wet and water-wet samples. In all these experiments, initially, the rock was exposed to the base fluids (SW or SW + IL) for 30 min before placing the droplet on the rock surface.

**3.1.2. Effect of Temperature and Pressure.** Subsequently, the temperature and pressure dependency of these studies were also analyzed. Figure 3 demonstrates the effect of temperature

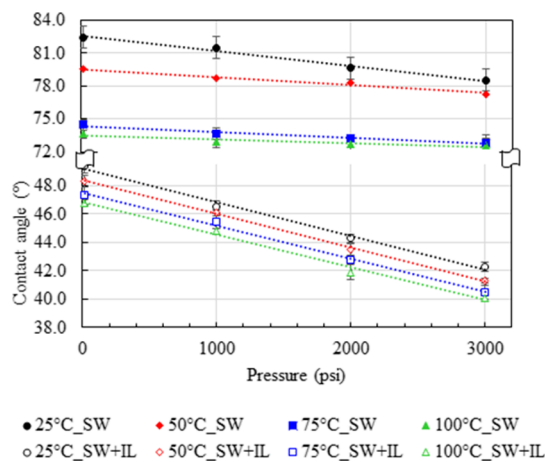


**Figure 3.** Temperature and pressure dependency on the static contact angle measurement of oil–rock–seawater systems with and without IL,  $[C_{12}mim]^+[Cl]^-$  (500 ppm), for the brine-saturated rock.

and pressure on the contact angle of rock–oil–seawater systems with and without ILs, 500 ppm of  $[C_{12}mim]^+[Cl]^-$ . We employed the brine-saturated rock sample for this case. Four different temperatures (25, 50, 75, and 100 °C) and pressures (14.7, 1000, 2000, and 3000 psig) were screened. A slightly decreasing trend was noted in the contact angle with increasing temperature and pressure, regardless of IL addition. For instance, the rock–oil–seawater system shows a contact angle

of 82.5° at 25 °C and in 14.7 psi, when increasing the temperature of the system to 100 °C; at the same pressure, it was found to be decreased to 73.6° (Figure 3). Similarly, on increasing the pressure of the system to 3000 psig at the same temperature, it was reduced as 78.5°, which is relatively a minor effect than the temperature. In the same way, the dependency of temperature and pressure was also studied on the rock–oil–seawater system with the addition of ILs and observed the reduction of contact angle from 49.4 to 42.3° with the increase of temperature from 25 to 100 °C at a constant pressure (14.7 psi). The pressure dependency was noted as 49.4–42.3 °C while increasing the pressure from 14.7 to 3000 psi, which is again very minor when compared to the temperature effect. Similar observations were also noticed for all other temperatures and pressures.

Correspondingly, identical experiments were conducted for the oil-saturated sample with and without IL,  $[C_{12}mim]^+[Cl]^-$ , for the dependency of temperature and pressure and are presented in Figure 4. The measured contact angle of the oil-

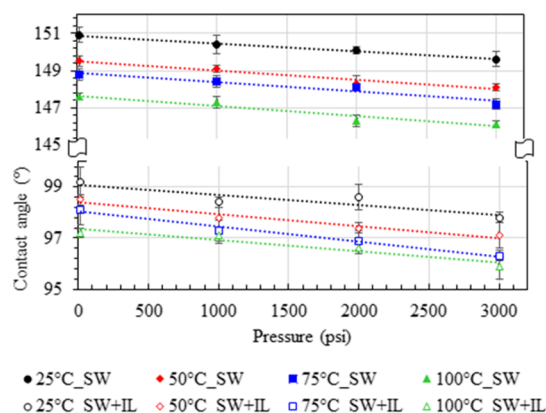


**Figure 4.** Temperature and pressure dependency on the static contact angle measurement of oil–rock–seawater systems with and without IL,  $[C_{12}mim]^+[Cl]^-$  (500 ppm), for the oil-saturated rock.

saturated rock–oil–seawater system was noted as 150.9° at the atmospheric conditions (25 °C and 14.7 psig), which indicates that the sample is in a highly oil-wet condition and gets reduced to 147.6° upon increasing the temperature of the system to 100 °C at the same pressure. Similarly, the increase of pressure from 14.7 to 3000 psig at the same temperature (25 °C) has dropped the contact angle slightly to 149.6 from 150.9°. The same study was repeated for the IL-added rock–oil–seawater system, and the changes of wettability were observed from 99.2 to 97.2 °C with an increase of temperature from 25 to 100 °C (at 14.7 psi). Similarly, when increasing the pressure of the system from 14.7 to 3000 psi at a constant temperature of 25 °C, the changes in the contact angle were shifted from 99.2 to 97.8 °C.

The temperature dependence of the wettability alterations (rock/oil/water three-phase interfacial interactions) is being influenced by various factors, such as, ions in the brine, ionic composition, pH, viscosity, relative permeability, oil–water IFT, thermal expansion, density, buoyancy effect, thin-film stability, and so forth. The temperature dependence of the oil–water relative permeability in the porous media is the most extensively studied phenomenon in the literature.<sup>38</sup> It is noted to have a relative permeability shift on the right side with increased water saturation while increasing the system's temperature. It indicates that the water-phase relative permeability increases in the



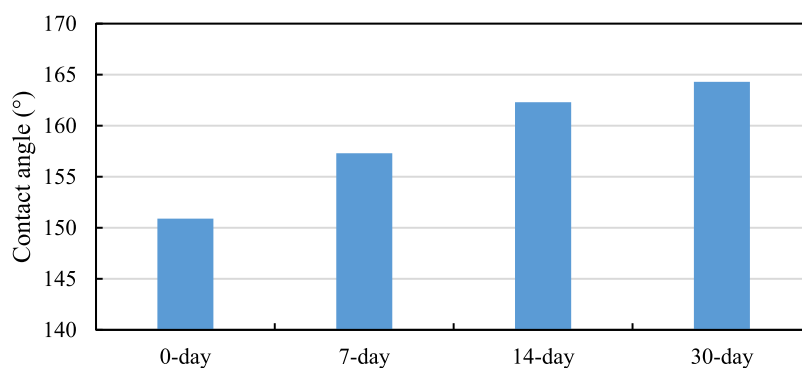


**Figure 5.** Effect of aging on the wettability measurements on the oil-saturated rock sample at 25 °C.

porous media with an increase in temperature. In addition, the decrease of the fluid's viscosity (intramolecular hydrogen bond reduction) while increasing the temperature could enhance the permeability of the fluids, particularly water relative permeability, which will invade on the pore as well as in the thin film at the three-phase interface. Besides, the oil–water interfacial tension also declines with an increase in system temperature, which indicates that the water resistance to flow in the three-phase interface (at the porous media surface) as well in the porous media is reduced by the capillary force. The dynamic motion of the ILs (increased particle collision) could also get increased while increasing the temperature, which will enhance the fluid's (water) pressure to a greater extent, leading to disjoining pressure.

Typically, the water (brine) film is found to be very weak in the oil-saturated core sample due to the hydrophobic interaction between the oil droplet and oil in the rock sample (deposited asphaltenes/resins), which in turn leads to rapid rupturing of the brine films. However, it can be tuned by altering the chemistry of the base fluids by introducing the ILs into the brine fluid. This will increase the brine film thickness at the three-phase interface even at harsh conditions, through various actions such as slower diffusion of ILs into the brine film, increasing disjoining pressure at the three-phase interline, increasing water-phase relative permeability, decreasing the viscosity of the base fluid, reduction of oil–water interfacial tension, and so forth.<sup>39</sup>

It is also revealed that the rock surface turns negative or less positive over an increase in temperature, repulsing the oil drops (organic components) and favoring the water-wet behavior.<sup>35</sup> It is understood that the combined effect of relative permeability, oil–water interfacial tension, IL diffusion into the thin film, and surface charges or potential variation over the temperature favors the increased water wetness than the lower temperature.

Overall, when increasing the temperature and pressure, the adhesive tendency of the crude oil on the rock surfaces was diminished significantly by increasing the cohesive nature of the oil. Moreover, the effect of pressure has the least domination<sup>40–42</sup> than the temperature.<sup>43–45</sup> However, the percentage of the reduction in the contact angle (18.8%;  $\Delta\theta \approx 49.4\text{--}40.1^\circ$ ) is relatively high in the case of IL-added brine-saturated rock–oil–seawater system than the system without IL (12%;  $\Delta\theta \approx 82.5\text{--}72.6^\circ$ ) over the increase of temperature and pressure (see Figure 3). Similarly, in the case of oil-saturated rock–oil–seawater system, the IL-added system also shows a better percentage reduction of the contact angle ( $\approx 3.2\%$ ) than the neat system without IL ( $\approx 3\%$ ) over the increase of temperature and pressure. It indicates that the ILs are more proficient even at extreme temperatures and pressures.

**3.1.3. Effect of Aging.** Second, we investigated the effect of aging on the oil-saturated samples. The oil-saturated samples were aged for different time periods as 0 day, 7 days, 14 days, and 30 days and then studied for static wettability. Figure 5 shows the measured contact angle of the rock–oil–seawater system as a function of aging. It can be evidently seen that the increase of aging time increases the oil wetness to some extent. Herein, the wettability was shifted from 150.9 to 164.3° while increasing the aging time from 0 to 30 days. This shows the occurrence of asphaltene deposition on the rock surface, which tunes the surface in favor of more oil-wet characteristics.<sup>33</sup>

**3.1.4. Effect of ILs Alkyl Chain Length.** Third, the efficiency of four various ILs ( $[\text{C}_4\text{mim}]^+[\text{Cl}]^-$ ,  $[\text{C}_6\text{mim}]^+[\text{Cl}]^-$ ,  $[\text{C}_8\text{mim}]^+[\text{Cl}]^-$ , and  $[\text{C}_{12}\text{mim}]^+[\text{Cl}]^-$ ) with variation in alkyl chain lengths was studied for the static wettability on the brine-saturated sample. All these measurements were performed at 25 °C and in various pressures from 14.7 to 3000 psi. The concentrations of the ILs were set to be constant as 500 ppm for all these measurements. Figure 6 shows the impact of each ILs

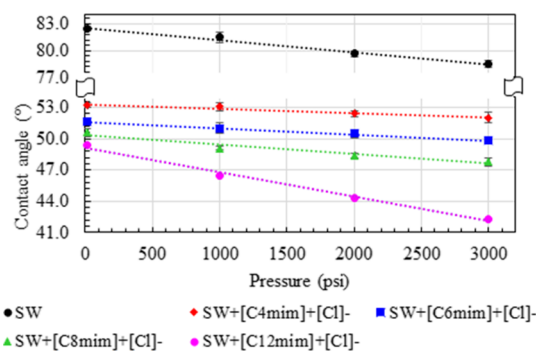


**Figure 6.** Effect of different ILs (500 ppm) on the static contact angle measurement of the rock–oil–seawater system for the brine-saturated rock at 25 °C.

on the measured static contact angle of the brine-saturated sample. It is very clear that the ILs had altered the wettability more significantly toward the strongly water-wet state. As can be seen in Figure 6, the increase of alkyl chain length on the cationic head of ILs is observed to be more efficient to increase the water wetness than the shorter chain containing ILs. It is to be noted that 500 ppm of  $[\text{C}_4\text{mim}]^+[\text{Cl}]^-$  reduces the contact angle from 82.5 to 53.2° at ambient conditions (25 °C and in 14.7 psig), whereas the addition of 500 ppm of  $[\text{C}_6\text{mim}]^+[\text{Cl}]^-$ ,  $[\text{C}_8\text{mim}]^+[\text{Cl}]^-$ , and  $[\text{C}_{12}\text{mim}]^+[\text{Cl}]^-$  reduces the contact angle to 51.6, 50.6, and 49.4°, respectively, at the same experimental conditions. It indicates that the increase of the

alkyl chain length increases their efficacy more significantly than the shorter chain containing ILs. It may be attributed to their difference in surface chemistry (charge of interactions) involved between the IL–oil and IL–carbonate rock interactions. In order to understand the mechanistic response of this IL-aided wettability alteration, we studied the measurement of  $\zeta$ -potential for various systems and reported at the later part of this study.

**3.1.5. Effect of Salinity.** In the last part of this section, we studied the efficiency of ILs over different salinity since most of the gulf reservoirs are highly salty with a huge composition of both mono and divalent ions. Also, most of the conventional chemical agents fail to withstand their colloidal stability at high salinity and further lose their efficacy in the process of wettability alteration due to their harsh environment. Therefore, we intended to screen the ILs at various saline mediums. In this study, we formulated three different brine fluids (SW, LS, and FW) at varying salt compositions (refer to Table 3) and studied them with IL,  $[C_{12}mim]^+[Cl]^-$ , to comprehend the IL performance on the wettability alteration at a wider range of salinity. Figure 7 shows the effect of IL,  $[C_{12}mim]^+[Cl]^-$ , on the

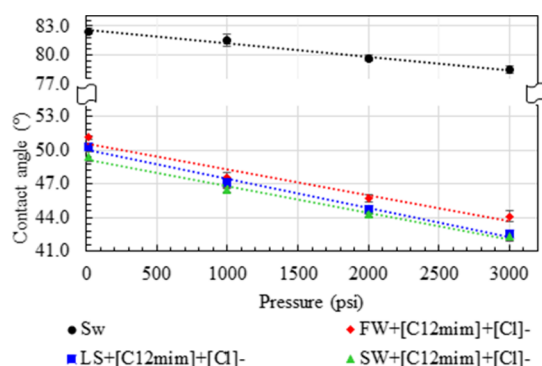


**Figure 7.** Effect of different salinity on the static contact angle measurement of the oil–rock–seawater system with and without IL,  $[C_{12}mim]^+[Cl]^-$ , for the brine-saturated rock at 25 °C.

contact angle study of the brine-saturated rock–oil–seawater system at three different salinity as SW (67,500 ppm), LS (138,000 ppm), and FW (241,000 ppm) at 25 °C, and in 14.7–3000 psi pressure. Overall, the performance of the IL was found to be more efficient regardless of any salinity. As can be seen in Figure 7, a slight increase in contact angle was observed with the increase of salinity, but still, the differences are almost negligible. For instance, the contact angle was found to be increased to 51.1 from 49.4° upon increasing the salinity to FW from SW at ambient conditions. We also studied the same brine-saturated rock–oil–seawater system without ILs. It resulted in a similar trend that the contact angle was raised slightly to 85.5 from 82.5° while increasing the salinity to FW from SW. Though the differences seem negligible, it is to be noted that the increase of salinity enhances the oil-wet nature of the rock surfaces. It may

be attributed to the minor variation in the electrostatic repulsion or interaction of the oil–water and oil–rock interfaces. Probably, the interaction between the oil–rock system could be enhanced by adsorbing more  $Na^+/Ca^{2+}/Mg^{2+}$  ions at the rock–oil or oil–water interfaces. On the other hand, the increase of ionic strength on the bulk fluid would suppress the brine film thickness (electrical double layer) that exists in between the rock and oil. This would increase the rock–oil interaction; on account of this, the high salinity brine results in more oil wetness than the low salinity medium.<sup>36</sup> This is detailed at the later part of this study by measuring the  $\zeta$ -potential. However, ILs were found to be more efficient and more stable regardless of any salinity. Therefore, ILs can be considered as the most appropriate candidate for harsh reservoir environments.

**3.2. Dynamic Wettability.** The dynamic wettability is the measurement of the contact angle that exists on the rock–oil–seawater system during the process of dynamic displacement of the base fluid with another fluid. This is the contact angle that exists when the surface tension at the contact line of the droplet is unbalanced or when the external force is applied to the droplet.<sup>46</sup> As mentioned in Section 2.2.2, this study focused on correlating this wettability dynamics measurement with the realistic flooding experiments. Figure 8 shows the effect of IL,  $[C_{12}mim]^+[Cl]^-$ , on the dynamic contact angle of the oil–saturated rock–oil–seawater system as a function of time up to 24 h at ambient conditions (25 °C, 14.7 psi). Initially, the contact angle of the rock–oil–seawater system was noted as 150.9°; later, seawater was displaced with 500 ppm of IL solution. Afterward, this system was retained for the next 24 h and monitored the transient changes in the contact angle. As expected, the contact angle of the system was altered more significantly from 150.9 to 118.5° over time; however, no significant change occurred on further extension of time duration beyond 24 h. It can be seen from Figure 8 that the diameter of the oil droplet was shrinking and dragging toward the base fluid as a result of dynamic changes of wettability. Though the contact angle was not dropped below 90°, it indicates that the angle changed toward weakly oil-wet state (118.5°), which is in fact a positive indication for the successful EOR. Moreover, on comparing the static and dynamic studies, it was noted that the static experiments show an excessive reduction in contact angle due to the pre-exposure of IL molecules on the rock surface. However, in the case of dynamic study, the IL molecules were introduced once we land the oil droplet on the rock surface, unlike the static measurements. This also implies that the mechanism of the static wettability is differing from the dynamic case. The simple adsorption of ILs on the rock surface could be the key factor in a static case. In the case of dynamics study, it could be attributed to the increase of structural disjoining pressure or the wedging tendency of the ILs on the rock–oil–water interphase.<sup>47</sup> Apart from this, capillary pressure reduction and higher interaction of the ILs on the rock surfaces than on oil would also make the rock surface to behave

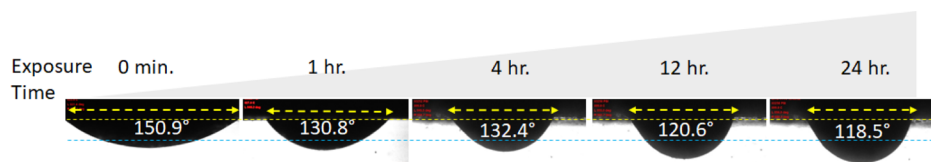


**Figure 8.** Effect of 500 ppm of IL,  $[C_{12}mim]^+[Cl]^-$ , on the dynamic contact angle of the oil–rock–seawater system at 25 °C for the oil-saturated rock for a period of 24 h.



as more of water wet. Though the contact angle reduction is relatively lesser in the dynamic experiments than the static method, this proves to be virtually more realistic and informative to correlate with the coreflood experiments. Furthermore, it is also important to investigate the adsorption studies of ILs in the porous media, which is in-planning to understand the level of rock–IL interactions and to quantify their loss during the EOR process.

**3.3. Interfacial Tension.** To support the wettability mechanism, we also measured the IFT of the oil–water systems with the addition of different chemicals as shown in Table 5. All

**Table 5. Measurement of Oil–Seawater Interfacial Tension with the Addition of ILs and Surfactants<sup>a</sup>**

sample	system	IFT (mN/m)	
		25 °C	100 °C
1	seawater (SW)	23.34	20.15
2	10 ppm [C <sub>12</sub> mim] <sup>+</sup> [Cl] <sup>-</sup> + SW	18.5	15.89
3	50 ppm [C <sub>12</sub> mim] <sup>+</sup> [Cl] <sup>-</sup> + SW	16.3	14.36
4	100 ppm [C <sub>12</sub> mim] <sup>+</sup> [Cl] <sup>-</sup> + SW	15.3	13.18
5	250 ppm [C <sub>12</sub> mim] <sup>+</sup> [Cl] <sup>-</sup> + SW	13.8	10.95
6	500 ppm [C <sub>12</sub> mim] <sup>+</sup> [Cl] <sup>-</sup> + SW	11.3	9.78
7	500 ppm [C <sub>8</sub> mim] <sup>+</sup> [Cl] <sup>-</sup> + SW	11.7	10.02
8	500 ppm [C <sub>6</sub> mim] <sup>+</sup> [Cl] <sup>-</sup> + SW	12.3	10.23
9	500 ppm [C <sub>4</sub> mim] <sup>+</sup> [Cl] <sup>-</sup> + SW	12.8	10.65
10	500 ppm AOS + SW	4.75	4.13
11	500 ppm [C <sub>12</sub> mim] <sup>+</sup> [Cl] <sup>-</sup> + 500 ppm AOS + SW	5.25	4.39

<sup>a</sup>The standard uncertainties are  $u(\text{IFT}) = 0.15$  mN/m and  $u(\text{ILs/AOS conc.}) = 2$  ppm.

these tests were performed at both 25 and 100 °C. As can be seen in Table 5, the increase of IL, [C<sub>12</sub>mim]<sup>+</sup>[Cl]<sup>-</sup>, concentration decreases the IFT more substantially to 11.3 from 23.34 mN/m, which is about 52% of the reduction recorded for the addition of 500 ppm of ILs. This implies that the IL molecules get arranged or positioned at the oil–water interfaces by the typical electrostatic interactions between the acidic component of oil (or the heteroatom of oil, –N, –O, and –S) with the cationic moiety of ILs. Usually, the ILs are freely soluble in the water phase due to their high hydrophilicity, and

they possess positive charges, which will interact with the oil interface electrostatically, thereby reducing the oil–water IFT. A similar study was performed for the 500 ppm of AOS surfactant, and it was noted that the IFT was reduced more effectively to 4.75 from 23.34 mN/m. This reduction of the IFT was more convinced than the IL system due to its better surfactant property. With our interest, we also determined for the combination of ILs and AOS (500 ppm of AOS and 500 ppm of [C<sub>12</sub>mim]<sup>+</sup>[Cl]<sup>-</sup>) with crude oil; interestingly, it was noted that there was a slight increment in the IFT. This could be attributed to the competitiveness of ILs and AOS for the arrangement at the oil–water interfaces; probably, the number of AOS availability at the interface would have been reduced by the IL placements.

In general, two types of classical mechanisms are reported in literature for the typical surfactant or nanofluid EOR, in which one is oil–water interfacial tension reduction and another one is the wettability alteration. Nevertheless, in our present study on ILs, we witnessed both the IFT reduction and wettability alteration. However, the wettability alteration is more dominant than the IFT reduction. As Wasan and Nikolov (2003) studied the nanofluid wettability dynamics, we can also extrapolate a similar approach for the IL case in our study.<sup>47</sup> Here, the diffusion of ILs into the rock–oil–brine system could have generated a kind of IL layers or a wedge film on the rock–oil–brine interface (at the three-phase contact line). This would facilitate the increase of the disjoining pressure on the three-phase interline; therefore, the alteration of wettability or contact angle would take place more toward the water-wet system. Additionally, the IL adsorption on the oil–water interfaces will reduce the interfacial tension, which further facilitates capillary pressure reduction. This indicates that the pressure of the wetting phase (ILs) is increased or the pressure of the non-wetting phase (oil) is decreased, due to which the wetting fluid spreads faster onto the rock surface than the non-wetting fluid.<sup>47–51</sup> Therefore, it is demonstrated that the ILs are capable of altering the rock–oil–brine wettability to the water-wet system through capillary pressure reduction and disjoining pressure increment.

**3.4. Zeta Potential.** In this section, we measured the  $\zeta$ -potential of some of the colloidal dispersions to understand the physicochemical interaction of the rock–oil–brine system with

**Table 6.  $\zeta$ -Potential Measurement of Different Colloidal Systems at Ambient Conditions<sup>a</sup>**

sample	systems	$\zeta$ -potential (mV)			
		25 °C		80 °C	
		without oil	with oil	without oil	with oil
1	DI water		–2.12		–2.01
2	DI + rock	–0.96	+0.18	–0.64	+0.11
3	DI + 500 ppm [C <sub>12</sub> mim] <sup>+</sup> [Cl] <sup>-</sup> + rock	+7.89	+3.87	+7.33	+3.42
4	SW		+4.80		+4.51
5	SW + rock	+18.8	+12.05	+18.25	+11.72
6	SW + 500 ppm [C <sub>12</sub> mim] <sup>+</sup> [Cl] <sup>-</sup>		+54.55		+54.38
7	SW + rock + 500 ppm [C <sub>12</sub> mim] <sup>+</sup> [Cl] <sup>-</sup>	+58.96	+48.36	+58.55	+48.03
8	SW + 500 ppm [C <sub>8</sub> mim] <sup>+</sup> [Cl] <sup>-</sup>		+50.39		+49.45
9	SW + rock + 500 ppm [C <sub>8</sub> mim] <sup>+</sup> [Cl] <sup>-</sup>	+55.36	+46.33	+54.33	+44.96
10	SW + 500 ppm [C <sub>6</sub> mim] <sup>+</sup> [Cl] <sup>-</sup>		+48.45		+48.11
11	SW + rock + 500 ppm [C <sub>6</sub> mim] <sup>+</sup> [Cl] <sup>-</sup>	+53.82	+44.26	+53.13	+43.89
12	SW + 500 ppm [C <sub>4</sub> mim] <sup>+</sup> [Cl] <sup>-</sup>		+46.28		+45.90
13	SW + rock + 500 ppm [C <sub>4</sub> mim] <sup>+</sup> [Cl] <sup>-</sup>	+51.71	+41.95	+51.25	+41.59

<sup>a</sup>The standard uncertainties are  $u(\zeta) = 0.1$  mV and  $u(\text{temperature}) = 0.2$  °C.

and without ILs. First, various sets of colloidal dispersions were prepared with different additives (rock, ILs, and oil), and then their  $\zeta$ -potential was determined using the Dispersion Tech Inc instrument. Table 6 shows the determined  $\zeta$ -potential of various samples with and without oil. It is noticed from Table 6 that the clean carbonate rock in deionized (DI) water was found to be relatively less negative as  $-0.96$  mV due to very less solubility of  $\text{CaCO}_3$  in water due to which the production of  $\text{CO}_3^{2-}$  will also be very less.<sup>42</sup> In the case of 500 ppm of IL + rock in DI, the  $\zeta$ -potential was recorded as  $+7.89$  mV due to the cationic imidazolium adsorption on the rock surfaces. The same system with the addition of oil slightly reduced the  $\zeta$ -potential to  $+3.87$  from  $+7.89$  mV, which indicates that the acidic fraction of the oil (negative charges) consumes some of the imidazolium cations that obviously limit the number of available imidazolium cations at the diffusive layer of the rock surface.

The same study was repeated with seawater to understand the impact of ILs on harsh environments. As shown in Table 6, the colloidal dispersion of the rock powder in seawater has resulted in the  $\zeta$ -potential as  $+18.8$  mV. This sudden increment of the potential indicates the adsorption of  $\text{Na}^+/\text{Ca}^+/\text{Mg}^+$  ions (a large quantity of mono- and divalent ions are composed in seawater composition) on the calcite rock surfaces; this strong accumulation of ions on the rock surfaces will form the strong double layer with positive nature.<sup>42,52</sup> As observed before, the addition of oil on the SW + rock system reduces the  $\zeta$ -potential to  $+12.05$  from  $+18.8$  mV. For the case of SW + 500 ppm of  $[\text{C}_{12}\text{mim}]^+[\text{Cl}]^-$  with oil, its  $\zeta$ -potential was found to have surged to as high as  $+54.55$  mV, which is much higher than the neat SW + rock + oil system. This indicates the strong adsorption or the interaction of imidazolium cations on the oil droplet surfaces along with the  $\text{Na}^+/\text{Ca}^+/\text{Mg}^+$  ions from SW. Finally, in the case of SW + 500 ppm of  $[\text{C}_{12}\text{mim}]^+[\text{Cl}]^-$  + rock, which was studied with and without oil, a potential of  $+58.96$  mV without oil and  $+48.36$  mV with oil was observed. This again shows that the extended adsorption of imidazolium cations and  $\text{Na}^+/\text{Ca}^+/\text{Mg}^+$  ions on the rock surfaces witnessed higher  $\zeta$ -potential as  $+58.96$  mV. As expected with the addition of oil, it was reduced to some extent as  $+58.36$  mV since the positive species ( $\text{Na}^+/\text{Ca}^+/\text{Mg}^+$ ) at the rock surfaces would have been reduced by their adsorption to the oil interface.<sup>42</sup> Overall, the addition of oil in all these cases showed a drop in the  $\zeta$ -potential, which could be due to the negative nature of the crude oil's resin/asphaltene.<sup>42</sup>

In general, these  $\zeta$ -potential determining experiments help to understand the complex microscopic interactions of the rock–oil–brine (three phases) systems. These interaction studies were further correlated with the wettability of the rock–oil–brine system to understand the wettability alteration mechanism. Herein, a thin brine film might exist between the rock and oil; however, depending on the type of interaction between rock, oil, and brine, this thin film may increase or decrease. Figure 9 shows the correlation between the measured contact angle and the  $\zeta$ -potential of the rock–oil–seawater system with and without IL,  $[\text{C}_{12}\text{mim}]^+[\text{Cl}]^-$ . It can be seen from Figure 9 that the  $\zeta$ -potential difference between the oil in seawater and rock in seawater,  $[\zeta_o - \zeta_r]$ , drops from 14 to 4.41 mV with the addition of ILs. This demonstrates the strong repulsion between the oil and rock with the addition of ILs. It is clear that the measured  $\zeta$ -potentials are in line with the contact angle experiments. Therefore, the ILs increase the interaction with oil (IFT reduction) and also on the rock surface, which help to decrease the rock–oil interaction to establish the rock matrix wettability

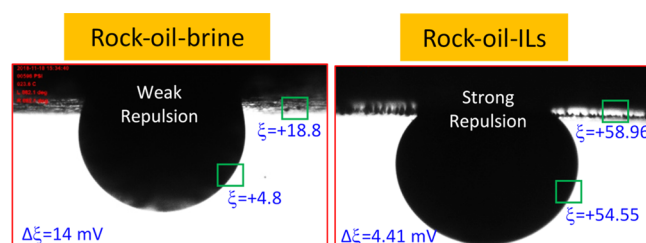


**Figure 9.** Illustration of the measured  $\zeta$ -potential values on their corresponding rock–oil–brine system with and without ILs.

alteration. Hence, it can be understood that the addition of ILs has the potency to alter the oil-wet rock matrix into a water-wet matrix even with a minor concentration of ILs. On the other hand, as can be seen in Table 6, the  $\zeta$ -potential difference between oil in SW and rock in SW,  $[\zeta_o - \zeta_r]$ , decreases from 5.43 to 4.41 mV when increasing the alkyl chain length of ILs from  $[\text{C}_4\text{mim}]^+[\text{Cl}]^-$  to  $[\text{C}_{12}\text{mim}]^+[\text{Cl}]^-$ . However, the neat system with no ILs was noted as  $[\zeta_o - \zeta_r] = 14.1$  mV. Therefore, obviously, the lesser the  $\Delta\zeta$  is, the better the wettability modification is. Thus, the increase of the alkyl chain length increases the hydrophobicity, which obviously shifts the  $\zeta$ -potential more toward the positive magnitude (refer to Table 6). Therefore, the presence of longer alkyl chain ILs would obviously increase their tendency repulsion between the rock and brine (ILs).

#### 4. CONCLUSIONS

In the present study, we have investigated the efficacy of four different imidazolium ILs (with varying alkyl chain lengths on the cationic head) on the wettability by measuring both the static and dynamic contact angles. In this study, we investigated several factors, such as the type of rock (brine-saturated and oil-saturated), type of IL, IL concentrations (0–500 ppm), aging, salinity (67,500–240,000 ppm), temperature (25–100 °C), and pressure (14.7–3000 psi). In the case of static wettability studies of brine-saturated rock–oil–seawater system, the wetting characteristic of the rock matrix was altered from neutral-wet to strongly water-wet (from 85.5 to 49.4°) upon adding 500 ppm of IL,  $[\text{C}_{12}\text{mim}]^+[\text{Cl}]^-$ . Similarly, for the oil-saturated rock–oil–seawater system, the wetness was altered to neutral-wet from strongly oil-wet (from 150.9 to 99.2°) for the same IL addition. However, in the case of dynamic study of the oil-saturated rock–oil–seawater system, the wettability was modified from strongly oil-wet to weakly oil-wet or neutral-wet (from 150.9 to 118.5°) upon displacing the native base fluid (seawater) with 500 ppm of IL,  $[\text{C}_{12}\text{mim}]^+[\text{Cl}]^-$ . Though it has relatively lesser effect as compared to the static experiment, this could be considered more realistic to correlate with the coreflood wettability studies. All these experiments were studied at extended pressures (14.7–3000 psig) and temperatures (25–100 °C) and a minor reduction on the measured contact angle was observed while increasing the temperature and pressure. The combined mechanistic actions of the various factors, such as interfacial tension reduction, disjoining pressure, capillary pressure alterations, and IL interactions, with the rock–oil–water interphase could have caused the wettability modification. In addition to this,  $\zeta$ -potential measurements of SW + rock and SW + IL + rock systems were performed with and without oil. The  $\zeta$ -potential analysis reveals that the ILs help to increase the rock–oil repulsions more significantly by the formation of a stronger electrical double layer on both the oil droplet and rock

surface by adsorbing more ILs on the surfaces. Conclusively, the results of the various experiments performed in this study are more impressive and favorable toward the EOR operation at high temperature, high pressure, and high salinity.

## AUTHOR INFORMATION

### Corresponding Author

Sivabalan Sakthivel – Center for Integrative Petroleum Research (CIPR), College of Petroleum Engineering & Geosciences, King Fahd University of Petroleum and Minerals, Dhahran 31261, Saudi Arabia; [orcid.org/0000-0002-0738-2895](https://orcid.org/0000-0002-0738-2895); Phone: 966 (013) 860-3917; Email: [sivabalan.sakthivel@kfupm.edu.sa](mailto:sivabalan.sakthivel@kfupm.edu.sa)

Complete contact information is available at:

<https://pubs.acs.org/10.1021/acsomega.1c02813>

### Notes

The author declares no competing financial interest.

## ACKNOWLEDGMENTS

The authors would like to acknowledge the Center for Integrative Petroleum Research, KFUPM, for the laboratory facility.

## REFERENCES

- (1) Nilsson, S.; Lohne, A.; Veggeland, K. Effect of Polymer on Surfactant Floodings of Oil Reservoirs. *Colloids Surf., A* **1997**, *127*, 241–247.
- (2) Aslan, S.; Fathi Najafabadi, N.; Firoozabadi, A. Non-monotonicity of the Contact Angle from NaCl and MgCl<sub>2</sub> Concentrations in Two Petroleum Fluids on Atomistically Smooth Surfaces. *Energy Fuels* **2016**, *30*, 2858–2864.
- (3) Najafi-Marghmaleki, A.; Barati-Harooni, A.; Soleymanzadeh, A.; Samadi, S. J.; Roshani, B.; Yari, A. Experimental Investigation of Effect of Temperature and Pressure on Contact Angle of Four Iranian Carbonate Oil Reservoirs. *J. Pet. Sci. Eng.* **2016**, *142*, 77–84.
- (4) Jarraghan, K.; Seiedi, O.; Sheykhan, M.; Sefti, M. V.; Ayatollahi, S. Wettability Alteration of Carbonate Rocks by Surfactants: A Mechanistic Study. *Colloids Surf., A* **2012**, *410*, 1–10.
- (5) Aghajanzadeh, M. R.; Ahmadi, P.; Sharifi, M.; Riazi, M. Wettability Modification of Oil-Wet Carbonate Reservoirs Using Silica-Based Nanofluid: An Experimental Approach. *J. Pet. Sci. Eng.* **2019**, *178*, 700–710.
- (6) Mohammed, M.; Babadagli, T. Wettability Alteration: A Comprehensive Review of Materials/Methods and Testing the Selected Ones on Heavy-Oil Containing Oil-Wet Systems. *Adv. Colloid Interface Sci.* **2015**, *220*, 54–77.
- (7) Welton, T. Room-Temperature Ionic Liquids. Solvents for Synthesis and Catalysis. *Chem. Rev.* **1999**, *99*, 2071–2084.
- (8) Plechkova, N. V.; Seddon, K. R. Applications of Ionic Liquids in the Chemical Industry. *Chem. Soc. Rev.* **2008**, *37*, 123–150.
- (9) Velusamy, S.; Sakthivel, S.; Gardas, R. L.; Sangwai, J. S. Substantial Enhancement of Heavy Crude Oil Dissolution in Low Waxy Crude Oil in the Presence of Ionic Liquid. *Ind. Eng. Chem. Res.* **2015**, *54*, 7999–8009.
- (10) Painter, P.; Williams, P.; Lupinsky, A. Recovery of Bitumen from Utah Tar Sands Using Ionic Liquids. *Energy Fuels* **2010**, *24*, 5081–5088.
- (11) Hasan, S. W.; Ghannam, M. T.; Esmail, N. Heavy Crude Oil Viscosity Reduction and Rheology for Pipeline Transportation. *Fuel* **2010**, *89*, 1095–1100.
- (12) Hogshead, C. G.; Manias, E.; Williams, P.; Lupinsky, A.; Painter, P. Studies of Bitumen–Silica and Oil–Silica Interactions in Ionic Liquids. *Energy Fuels* **2011**, *25*, 293–299.
- (13) Pillai, P.; Kumar, A.; Mandal, A. Mechanistic Studies of Enhanced Oil Recovery by Imidazolium-Based Ionic Liquids as Novel Surfactants. *J. Ind. Eng. Chem.* **2018**, *63*, 262–274.
- (14) Pillai, P.; Mandal, A. A Comprehensive Micro Scale Study of Poly-Ionic Liquid for Application in Enhanced Oil Recovery: Synthesis, Characterization and Evaluation of Physicochemical Properties. *J. Mol. Liq.* **2020**, *302*, 112553.
- (15) Sakthivel, S.; Velusamy, S.; Gardas, R. L.; Sangwai, J. S. Adsorption of aliphatic ionic liquids at low waxy crude oil-water interfaces and the effect of brine. *Colloids Surf., A* **2015**, *468*, 62–75.
- (16) Sakthivel, S.; Velusamy, S.; Gardas, R. L.; Sangwai, J. S. Eco-Efficient and Green Method for the Enhanced Dissolution of Aromatic Crude Oil Sludge Using Ionic Liquids. *RSC Adv.* **2014**, *4*, 31007–31018.
- (17) Sakthivel, S.; Velusamy, S.; Gardas, R. L.; Sangwai, J. S. Use of Aromatic Ionic Liquids in the Reduction of Surface Phenomena of Crude Oil-Water System and Their Synergism with Brine. *Ind. Eng. Chem. Res.* **2015**, *54*, 968–978.
- (18) Sakthivel, S.; Velusamy, S.; Gardas, R. L.; Sangwai, J. S. Experimental Investigation on the Effect of Aliphatic Ionic Liquids on the Solubility of Heavy Crude Oil Using UV-Visible, Fourier Transform-Infrared, and <sup>13</sup>C NMR Spectroscopy. *Energy Fuels* **2014**, *28*, 6151–6162.
- (19) Sakthivel, S.; Velusamy, S.; Gardas, R. L.; Sangwai, J. S. Nature Friendly Application of Ionic Liquids for Dissolution Enhancement of Heavy Crude Oil. *Proceedings—SPE Annual Technical Conference and Exhibition*; Janua, 2015; Vol. 2015.
- (20) Sakthivel, S.; Chhotaray, P. K.; Velusamy, S.; Gardas, R. L.; Sangwai, J. S. Synergistic Effect of Lactam, Ammonium and Hydroxyl Ammonium Based Ionic Liquids with and without NaCl on the Surface Phenomena of Crude Oil/Water System. *Fluid Phase Equilib.* **2015**, *398*, 80–97.
- (21) Sakthivel, S.; Gardas, R. L.; Sangwai, J. S. Spectroscopic Investigations to Understand the Enhanced Dissolution of Heavy Crude Oil in the Presence of Lactam, Alkyl Ammonium and Hydroxyl Ammonium Based Ionic Liquids. *J. Mol. Liq.* **2016**, *221*, 323–332.
- (22) Sakthivel, S.; Gardas, R. L.; Sangwai, J. S. Effect of Alkyl Ammonium Ionic Liquids on the Interfacial Tension of the Crude Oil-Water System and Their Use for the Enhanced Oil Recovery Using Ionic Liquid-Polymer Flooding. *Energy Fuels* **2016**, *30*, 2514–2523.
- (23) Velusamy, S.; Sakthivel, S.; Sangwai, J. S. Effect of Imidazolium-Based Ionic Liquids on the Interfacial Tension of the Alkane-Water System and Its Influence on the Wettability Alteration of Quartz under Saline Conditions through Contact Angle Measurements. *Ind. Eng. Chem. Res.* **2017**, *56*, 13521–13534.
- (24) Velusamy, S.; Sakthivel, S.; Neelakantan, L.; Sangwai, J. S. Imidazolium-Based Ionic Liquids as an Anticorrosive Agent for Completion Fluid Design. *J. Earth Sci.* **2017**, *28*, 949–961.
- (25) Sakthivel, S.; Velusamy, S.; Nair, V. C.; Sharma, T.; Sangwai, J. S. Interfacial Tension of Crude Oil-Water System with Imidazolium and Lactam-Based Ionic Liquids and Their Evaluation for Enhanced Oil Recovery under High Saline Environment. *Fuel* **2017**, *191*, 239–250.
- (26) Velusamy, S.; Sakthivel, S.; Sangwai, J. S. Effects of Imidazolium-Based Ionic Liquids on the Rheological Behavior of Heavy Crude Oil under High-Pressure and High-Temperature Conditions. *Energy Fuels* **2017**, *31*, 8764–8775.
- (27) Pillai, P.; Pal, N.; Mandal, A. Synthesis, Characterization, Surface Properties and Micellization Behaviour of Imidazolium-Based Ionic Liquids. *J. Surfactants Deterg.* **2017**, *20*, 1321–1335.
- (28) Sakthivel, S.; Velusamy, S. Eco-Efficient Rheological Improvement of Heavy Crude Oil Using Lactam Based Ionic Liquids at High Temperature High Pressure Condition. *Fuel* **2020**, *276*, 118027.
- (29) Bin Dahbag, M.; AlQuraishi, A.; Benzagouta, M. Efficiency of Ionic Liquids for Chemical Enhanced Oil Recovery. *J. Pet. Explor. Prod. Technol.* **2015**, *5*, 353–361.
- (30) Cao, N.; Mohammed, M. A.; Babadagli, T. Wettability Alteration of Heavy-Oil-Bitumen-Containing Carbonates by Use of Solvents, High-PH Solutions, and Nano/Ionic Liquids. *SPE Reservoir Eval. Eng.* **2017**, *20*, 363–371.



- (31) Nabipour, M.; Ayatollahi, S.; Keshavarz, P. Application of Different Novel and Newly Designed Commercial Ionic Liquids and Surfactants for More Oil Recovery from an Iranian Oil Field. *J. Mol. Liq.* **2017**, *230*, 579–588.
- (32) Abdullah, M. M. S.; AlQuraishi, A. A.; Allohedan, H. A.; AlMansour, A. O.; Atta, A. M. Synthesis of Novel Water Soluble Poly (Ionic Liquids) Based on Quaternary Ammonium Acrylamidomethyl Propane Sulfonate for Enhanced Oil Recovery. *J. Mol. Liq.* **2017**, *233*, 508–516.
- (33) Kanj, M.; Sakthivel, S.; Giannelis, E. Wettability Alteration in Carbonate Reservoirs by Carbon Nanofluids. *Colloids Surf., A* **2020**, *598*, 124819.
- (34) Mohammadi, M.; Mahani, H. Direct Insights into the Pore-Scale Mechanism of Low-Salinity Waterflooding in Carbonates Using a Novel Calcite Microfluidic Chip. *Fuel* **2020**, *260*, 116374.
- (35) Mahani, H.; Menezes, R.; Berg, S.; Fadili, A.; Nasralla, R.; Voskov, D.; Joekar-Niasar, V. Insights into the Impact of Temperature on the Wettability Alteration by Low Salinity in Carbonate Rocks. *Energy Fuels* **2017**, *31*, 7839–7853.
- (36) Pourakaberian, A.; Mahani, H.; Niasar, V. The Impact of the Electrical Behavior of Oil-Brine-Rock Interfaces on the Ionic Transport Rate in a Thin Film, Hydrodynamic Pressure, and Low Salinity Waterflooding Effect. *Colloids Surf., A* **2021**, *620*, 126543.
- (37) Drelich, J.; Fang, C.; White, C. L. Measurement of Interfacial Tension in Fluid-Fluid Systems. *Encyclopedia of Surface and Colloid Science*; Marcel Dekker Inc., 2002; Vol. 3, pp 3158–3163.
- (38) Rao, D. N. Wettability Effects in Thermal Recovery Operations. *SPE Reservoir Eval. Eng.* **1999**, *2*, 420–430.
- (39) Hamouda, A. A.; Karoussi, O.; Chukwudeme, E. A. Relative Permeability as a Function of Temperature, Initial Water Saturation and Flooding Fluid Compositions for Modified Oil-Wet Chalk. *J. Pet. Sci. Eng.* **2008**, *63*, 61–72.
- (40) Hjelmeland, O. S.; Larrondo, L. E. Experimental Investigation of the Effects of Temperature, Pressure, and Crude Oil Composition on Interfacial Properties. *SPE Reservoir Eng.* **1986**, *1*, 321–328.
- (41) Wang, W.; Gupta, A. Investigation of the Effect of Temperature and Pressure on Wettability Using Modified Pendant Drop Method. *SPE Annual Technical Conference and Exhibition*; Society of Petroleum Engineers, 1995.
- (42) Lu, Y.; Najafabadi, N. F.; Firoozabadi, A. Effect of Temperature on Wettability of Oil/Brine/Rock Systems. *Energy Fuels* **2017**, *31*, 4989–4995.
- (43) Tang, G. Q.; Morrow, N. R. Salinity, Temperature, Oil Composition, and Oil Recovery by Waterflooding. *SPE Reservoir Eng.* **1997**, *12*, 269–276.
- (44) McCaffery, F. G.; Bennion, D. W. The Effect Of Wettability On Two-Phase Relative Penneabilities. *J. Can. Pet. Technol.* **1974**, *13*, 42–53. DOI: 10.2118/74-04-04
- (45) Poston, S. W.; Ysrael, S.; Hossain, A. K. M. S.; Montgomery, E. F. The Effect of Temperature on Irreducible Water Saturation and Relative Permeability of Unconsolidated Sands. *Soc. Pet. Eng. J.* **1970**, *10*, 171–180.
- (46) Sefiane, K.; Skilling, J.; MacGillivray, J. Contact Line Motion and Dynamic Wetting of Nanofluid Solutions. *Adv. Colloid Interface Sci.* **2008**, *138*, 101–120.
- (47) Wasan, D. T.; Nikolov, A. D. Spreading of Nanofluids on Solids. *Nature* **2003**, *423*, 156–159.
- (48) Sofla, S. J. D.; James, L. A.; Zhang, Y. Toward a Mechanistic Understanding of Wettability Alteration in Reservoir Rocks Using Silica Nanoparticles. *E3S Web of Conferences*; EDP Sciences, 2019; Vol. 89, p 03004.
- (49) Zhang, H.; Nikolov, A.; Wasan, D. Enhanced Oil Recovery (EOR) Using Nanoparticle Dispersions: Underlying Mechanism and Imbibition Experiments. *Energy Fuels* **2014**, *28*, 3002–3009.
- (50) Kondiparty, K.; Nikolov, A. D.; Wasan, D.; Liu, K.-L. Dynamic Spreading of Nanofluids on Solids. Part I: Experimental. *Langmuir* **2012**, *28*, 14618–14623.
- (51) Mcelfresh, P. M.; Holcomb, D. L.; Ector, D. Application of Nanofluid Technology to Improve Recovery in Oil and Gas Wells. *SPE International Oilfield Nanotechnology Conference and Exhibition*; Society of Petroleum Engineers, 2012.
- (52) Chen, L.; Zhang, G.; Wang, L.; Wu, W.; Ge, J. Zeta Potential of Limestone in a Large Range of Salinity. *Colloids Surf., A* **2014**, *450*, 1–8.